Title

The Impact of COVID-19 on CO_2 Emissions in the Los Angeles and Washington DC/Baltimore Metropolitan Areas.

Journal

Geophysical research letters, 48(11)

ISSN

0094-8276

Authors

Yadav, Vineet
Ghosh, Subhomoy
Mueller, Kimberly
et al.

Publication Date

2021-06-01

DOI

10.1029/2021gl092744

Peer reviewed

Geophysical Research Letters

RESEARCH LETTER
10.1029/2021GL092744

Special Section:
The COVID-19 pandemic: linking health, society and environment

The Impact of COVID-19 on CO_2 Emissions in the Los Angeles and Washington DC/Baltimore Metropolitan Areas

Vineet Yadav[1], Subhomoy Ghosh[2,3], Kimberly Mueller[3], Anna Karion[3], Geoffrey Roest[4], Sharon M. Gourdji[3], Israel Lopez-Coto[3], Kevin R. Gurney[4], Nicholas Parazoo[1], Kristal R. Verhulst[1], Jooil Kim[5], Steve Prinzivalli[6], Clayton Fain[6], Thomas Nehrkorn[7], Marikate Mountain[7], Ralph F. Keeling[5], Ray F. Weiss[5], Riley Duren[8], Charles E. Miller[1], and James Whetstone[3]

[1]Jet Propulsion Laboratory, California Institute of Technology, Pasadena, CA, USA, [2]Center for Research Computing, University of Notre Dame, South Bend, IN, USA, [3]National Institute of Standards and Technology, Gaithersburg, MD, USA, [4]School of Informatics, Computing, and Cyber Systems, Northern Arizona University, Flagstaff, AZ, USA, [5]Scripps Institution of Oceanography, University of California, San Diego, La Jolla, CA, USA, [6]Earth Networks, Germantown, MD, USA, [7]Atmospheric and Environmental Research, Lexington, MA, USA, [8]Arizona Institutes for Resilience, The University of Arizona, Tucson, AZ, USA

Key Points:

- Atmospheric CO_2 observations can be used to detect the onset of the COVID-19 response in Los Angeles and Washington DC/Baltimore
- Relative reductions in April 2020 associated with COVID-19 are ~30% when compared to emissions in 2018 and 2019
- Decreases in vehicular traffic do not completely explain observed emissions reductions in both Los Angeles and Washington DC/Baltimore

Supporting Information:

Supporting Information may be found in the online version of this article.

Correspondence to:

K. Mueller,
Kimberly.Mueller@nist.gov

Citation:

Yadav, V., Ghosh, S., Mueller, K., Karion, A., Roest, G., Gourdji, S. M., et al. (2021). The impact of COVID-19 on CO_2 emissions in the Los Angeles and Washington DC/Baltimore metropolitan areas. *Geophysical Research Letters*, *48*, e2021GL092744. https://doi.org/10.1029/2021GL092744

Received 28 JAN 2021
Accepted 14 APR 2021

Abstract Responses to COVID-19 have resulted in unintended reductions of city-scale carbon dioxide (CO_2) emissions. Here, we detect and estimate decreases in CO_2 emissions in Los Angeles and Washington DC/Baltimore during March and April 2020. We present three lines of evidence using methods that have increasing model dependency, including an inverse model to estimate relative emissions changes in 2020 compared to 2018 and 2019. The March decrease (25%) in Washington DC/Baltimore is largely supported by a drop in natural gas consumption associated with a warm spring whereas the decrease in April (33%) correlates with changes in gasoline fuel sales. In contrast, only a fraction of the March (17%) and April (34%) reduction in Los Angeles is explained by traffic declines. Methods and measurements used herein highlight the advantages of atmospheric CO_2 observations for providing timely insights into rapidly changing emissions patterns that can empower cities to course-correct CO_2 reduction activities efficiently.

Plain Language Summary In this study, we use atmospheric CO_2 observations from urban measurement networks in Los Angeles and Washington DC/Baltimore to detect the onset of the pandemic response. We show that April 2020 emissions were ~30% lower than in previous years in both metropolitan areas. Decreases in vehicular traffic do not completely explain the observed emissions reductions, demonstrating the complex interplay of human activities and atmospheric dynamics that drive CO_2 emissions at the urban scale.

1. Introduction

Responses to public health threats presented by the global COVID-19 pandemic dramatically altered daily activities in cities around the world, including in the Los Angeles and Washington DC/Baltimore metropolitan areas. Researchers have attempted to determine the extent to which CO_2 emissions were impacted by the pandemic, linking changes in emissions to processes and sectors using different types of activity data and baselines for comparisons (Le Quéré et al., 2020; Liu et al., 2020; Zheng et al., 2020). One study shows that CO_2 emissions declined by 3.9% globally in the first 4 months in 2020, attributing half of this decline to changes in traffic and mobility (Le Quéré et al., 2020). Unlike these studies, which use only activity data to estimate declines, here we also use atmospheric CO_2 observations to detect when and how emissions were impacted, and focus on CO_2 emissions reductions at the city scale.

Our analysis relies on high-accuracy atmospheric CO_2 observations from urban networks, building on a recently published study that used lower-accuracy CO_2 sensors to estimate COVID-19 related impacts for the San Francisco Bay area (Turner et al., 2020). Here, we evaluate impacts in two separate metropolitan areas: Los Angeles and Washington DC/Baltimore, allowing for an inter-comparison between two large urban regions. In Los Angeles and Washington DC/Baltimore, traffic congestion and commuting play dominant

roles, yet each region has important differentiating characteristics related to its economy, infrastructure, climate, and demographics. As such, the impact of COVID-19 on CO_2 emissions is layered on top of other forces, for example, energy shifts or specific weather conditions, that drive emissions within these cities.

We take a comprehensive approach by exploring the full value of CO_2 observations for understanding events like COVID-19 that drive urban-scale emissions. The CO_2 observations are used in three distinct analyses with increasing model dependency. The first detects the timing of emissions declines using atmospheric CO_2 observations, the second evaluates CO_2 enhancements to assess the persistence of reduced emissions, and the third employs an inverse model to estimate the relative change in emissions in 2020 compared to 2018 and 2019. In addition to detecting the timing and estimating the magnitude of emissions declines using atmospheric CO_2 observations, we also examine proxy activity data to tease apart the influence of COVID-19 from other factors that impact emissions.

2. Site Descriptions

For this study, we consider Washington DC and Baltimore as a single metropolitan area (DC-Balt), given these cities' proximity and intersecting suburbs (US Census, 2010). We also focus on the wider metropolitan extent of the Los Angeles area (LA). While topographically very different, both regions are similar in size (~18,000 km^2) and are densely populated (Figure S3). The two regions experience very different climates: LA's is characterized by seasonal changes in rainfall with a dry summer and a rainy winter, while DC-Balt experiences hot, humid summers and cold, wet winters. These climatological differences impact emissions from heating and cooling as well as urban and surrounding vegetation, which controls CO_2 uptake and release from the biosphere.

The emissions magnitude and relative contribution of different sectors to emissions in each city reflect the economies in these metropolitan centers. Two existing 1 km^2 emissions data products give insight into sectoral distributions. Here we refer to the Hestia emissions product, tailored for LA (Gurney et al., 2019), and Vulcan 3.0 (Gurney et al., 2020), a national emissions product, in DC-Balt. The two emission products are constructed using similar methods and are consistent, such that the domain total for LA in the Vulcan national product is the same as in Hestia. According to these products, the total annual magnitude of in-boundary CO_2 emissions in LA is 43.7 megatons of carbon (MtC)/year, which is over twice that of DC-Balt, 20.5 MtC/year (Figure S1). Although each city has its own sectoral emission mix, the on-road sector dominates in both LA and DC-Balt, with on-road sector emissions accounting for ~45% of annual totals in both cities. The industrial sector is the second largest component in LA, accounting for an additional 23% of the yearly total. The electricity production sector in DC-Balt is the second most important contributor, accounting for 19% of annual emissions.

The sectoral breakdown of fossil-fuel CO_2 ($FFCO_2$) emissions in DC-Balt exhibit much larger seasonal and annual variability compared to LA due to regional climate and energy demand (Figure S1). The changes in emissions are evident during the transition from winter to spring, corresponding to our study period of January through May; DC-Balt emissions show wide ranges for the commercial (~23%–4%) and residential (~20%–4%) sector fractions due to reduced demand for heating in the warmer months compared with January and February (Figure S2).

3. Measurements

Both the LA and DC-Balt metropolitan areas are being monitored for ambient CO_2 levels using networks of high-accuracy measurement stations. Each network has ~9–13 sites with sensitivity to urban anthropogenic emissions (Figure S3; Tables S1 and S2), although the number of sites and measurements available in any given month varies, depending on how each network was developed and maintained (Karion et al., 2020; Kort et al., 2013; Lopez-Coto et al., 2017; Mueller et al., 2018; Verhulst et al., 2017). We use 2018 and 2019 as baseline years with which to compare 2020 observations and inferred emissions because we have a consistent number of observational sites for each domain during these times. The network sensitivity, or footprint, of the urban CO_2 measurements is also generally consistent in these 3 years (Figure S4). Although we do

not have a long-term record as a basis for comparison, using the average of two baseline years allows us to account for some year-to-year variability in emissions.

Atmospheric CO_2 observations from the two urban networks contain signatures from biospheric and anthropogenic CO_2 sources and sinks within the footprint, which can include fluxes from both inside and outside the urban domain. We define $FFCO_2$ as all fluxes that result from combustion. As such, isolating the $FFCO_2$ contribution to CO_2 observations from each urban domain requires an understanding of biospheric fluxes and incoming CO_2 (i.e., background).

Discerning $FFCO_2$-driven enhancements in LA is more straightforward than in DC-Balt because, in part, the biosphere has less of an impact (Miller et al., 2020). We use a non-year specific biospheric model, the Vegetation Photosynthesis Respiration Model (VPRM for July 2017 to June 2018 as described in Section S5.1.1; Figure S5a), to model the biological fluxes. Modeled biospheric enhancements are consistent at the city scale with those presented in Miller et al. (2020) from January to May. We use measurements from the site on San Clemente Island (SCI) to represent incoming airflow (Verhulst et al., 2017). Median monthly $FFCO_2$ enhancements estimated from atmospheric CO_2 observations within LA range between 8 μmol mol^{-1} and 30 μmol mol^{-1} (Section S6; Figure S6a).

Representing CO_2 concentration of incoming airflow for DC-Balt is more difficult because the domain is downwind of large agricultural areas, deciduous forests, and emission sources, including other metropolitan areas and power plants. We represent the incoming CO_2 based on observations from one of three near-boundary towers (BUC, SFD, or TMD, Figure S3) selected using modeled back-trajectories (described in Section S3.1) similar to a recent study in Boston (Karion et al., 2021; Sargent et al., 2018), and described further in Section S4.

In DC-Balt, we represent biospheric fluxes using year-specific (2018–2020) VPRM to ensure properly characterized variability in the modeled fluxes (Section S5.1.2). Average daily observed drawdown due to biological activity can be as high as 4.7 μmol mol^{-1} (as predicted by VPRM; Figure S5b) during our study period. After accounting for inflow and the contribution of biological fluxes to observed CO_2, the estimated median monthly $FFCO_2$ enhancements for DC-Balt are ∼1.5 μmol mol^{-1}–7 μmol mol^{-1} in January through May between 2018 and 2020, 3–4 times lower than those in LA (Figure S6).

4. Methods

We use three different types of analysis to detect the onset of the COVID-19 effect on CO_2 emissions and estimate the relative change of emissions. To simplify the interpretation of results, we keep most of the modeling and analysis components consistent between LA and DC-Balt. However, there are a few differences that cannot be avoided due to city-specific meteorology and availability of data. Our period of assessment includes the months of January–May for 2018, 2019, and 2020, with 2018 and 2019 observations and inferred emissions providing baselines for comparison with 2020.

For the first analysis, we focus on the temporal variability of measured atmospheric CO_2 rather than the concentrations themselves to detect the timing of emissions changes. CO_2 enhancements contain large variability associated with weather conditions, making it difficult to isolate changes, while high-frequency (sub-hourly scale) variability is expected to directly correlate with emissions near the observation locations and are less affected by synoptic conditions (Umezawa et al., 2020). To identify changes in variability in 2020 compared to previous years, we use the ratio of the standard deviations of the 1 min averages in 2020 to the averaged standard deviations from 2018 and 2019 in a change point analysis (Aminikhanghahi & Cook, 2017) (Section S6.1) and estimate dates associated with sudden emissions decline and recovery.

In the second analysis, we examine the atmospheric CO_2 observations by assessing the mean daily cumulative afternoon (i.e., the time period when the atmosphere is well-mixed) $FFCO_2$ enhancement, comparing 2020 to other years. We calculate $FFCO_2$ enhancements ($\mathbf{y}_{\mathbf{FFCO_2}}$) as follows:

$$\mathbf{y}_{\mathbf{FFCO_2}} = \mathbf{y}_{\mathbf{obs}} - \mathbf{y}_{\mathbf{back}} - \mathbf{y}_{\mathbf{bio}}, \quad (1)$$

$$\mathbf{y}_{\mathbf{bio}} = \mathbf{H}\mathbf{s}_{\mathbf{VPRM}}, \quad (2)$$

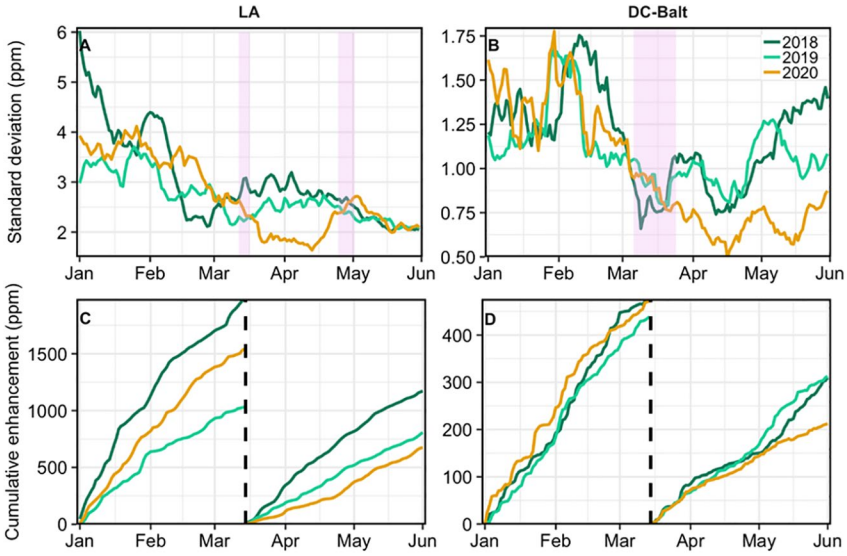

Figure 1. Moving 15-day average of daily afternoon network-wide means of the within-hour standard deviation for (a) LA and (b) DC-Balt, for three study years. Change point credible intervals are shaded pink. (c and d) Cumulative fossil-fuel CO_2 (FFCO2) enhancements (daily afternoon network-wide means) for each of the three years, starting on January 1 and re-starting on March 13 (black dashed line), the date associated with the behavioral shifts reflected in Apple mobility (Apple, 2020).

where $\mathbf{y_{obs}}$ are the CO_2 mole fractions in μmol CO_2 per mol of dry air, or ppm, as observed at the urban measurement sites; $\mathbf{y_{back}}$ is the background CO_2 (Section S4); $\mathbf{H}$, expressed in (μmol mol^{-1})/(μmol m^{-2} s^{-1}), represents sensitivities of the observations to surface fluxes as obtained from the atmospheric transport and dispersion model (Section S3.1); and $\mathbf{y_{bio}}$ are the biological contributions to $\mathbf{y_{obs}}$ as modeled through the convolution of $\mathbf{H}$ and the modeled VPRM fluxes ($\mathbf{s_{VPRM}}$; Section S5) with units μmol m^{-2} s^{-1}. Additional detail on the cumulative summation method is given in Section S6.2.

In the final analysis, we used a geostatistical-Bayesian atmospheric inverse modeling approach with $\mathbf{y_{FFCO_2}}$ as observations to estimate posterior $FFCO_2$ emissions. We use Hestia (LA) and a temporally smoothed Vulcan 3.0 (DC-Balt) emission product for 2015, the most recent year available for both products, as covariates (priors) in the two inversions. Both priors are re-gridded to 0.02° × 0.02° for the domains in Figure S3. To estimate the gridded posterior emissions, we adopt a moving window approach to estimate $FFCO_2$ emissions at daily temporal intervals by maintaining a one-day overlap between two 2-day inversions (for details see Section S7).

The posterior $FFCO_2$ emissions are used to detect a relative change in emissions in March and April of 2020 in comparison to the mean of the baseline years, 2018 and 2019. The posteriors are further compared against adjusted domain total $FFCO_2$ emissions from Hestia and Vulcan 3.0 computed using information on statewide fuel sales, continuous emissions monitoring systems (CEMS) data from powerplants, natural gas consumption, and vehicle miles traveled (VMT) data (Section S8).

5. Detection and Persistence of Emission Declines

The influence of the pandemic response on $FFCO_2$ emissions is evident in both the variability of concentrations (as indicated by their standard deviation) and the cumulative $FFCO_2$ enhancements in LA and DC-Balt (Figure 1). In the observation analysis, we observe a reduction in the standard deviation of CO_2 within each hour, averaged daily over all sites, in mid-March 2020 relative to 2018 and 2019 in both metropolitan areas suggesting that emissions declined substantially at that time (Figures 1a and 1b). The reduction in CO_2 variability is also apparent in the statistically significant smaller interquartile range of hourly averaged $\mathbf{y_{FFCO_2}}$ (Figure S6). The change points in the ratio of 2020 standard deviations to the averaged standard deviations from 2018 to 2019 were detected on March 14 (LA) and March 13 (DC-Balt), with lower 2020

standard deviations after these dates, matching the timing of behavioral shifts indicated in Apple mobility data (Apple, 2020). The corresponding uncertainties as indicated by the 95% credible intervals (Section S6.1) are 6 days (LA) and 21 days (DC-Balt). We also detect a second change point for LA on April 29 with a 95% credible interval of 9 days, associated with an increase in traffic (Figures 1a and S11) (California Dept. of Transportation, 2020). Uncertainty bounds in LA are narrower due to the sharper relative drop in the standard deviation. We did not detect a second change point in the DC-Balt data, perhaps due to the ramp-up of the biosphere during this time period.

The transition in LA is also evident when comparing the $FFCO_2$ cumulative enhancements before and after the decrease in mobility (Figure 1c). Large interannual variability of the cumulative enhancements in LA is likely due to climatological or other extreme atmospheric events like a fire in early 2018. However, the reduced $FFCO_2$ cumulative enhancements after March 13, 2020 relative to 2018 and 2019 are apparent. Evaluating LA cumulative enhancements over additional years (2015–2020; Figure S7), we find that 2020 enhancements prior to March 13 are well within interannual variability, further indicating that the low post-March 13 enhancements in 2020 are likely caused by an emission change rather than year-specific meteorological variability.

In DC-Balt, the 2020 cumulative enhancement is slightly higher in the beginning of the year than in 2018 and 2019 (Figure 1d). After March 13, 2020 cumulative enhancements are lower than the previous 2 years, again indicating a change in emissions although less apparent than for LA. There may be several reasons why the $\mathbf{y}_{\mathbf{FFCO_2}}$ decrease in 2020 is not larger, including lower overall enhancements in DC-Balt compared to LA (leading to smaller signals) or interannual differences in transport, which affect the relationship between enhancements and emissions. However, despite the difference in magnitude between the cities, at the onset of behavioral shifts (~March 13, dashed vertical line in Figures 1c and 1d), the enhancement growth for 2020 is lower suggesting a decrease in emissions—a conclusion consistent with the results of the LA $FFCO_2$ enhancement analysis.

6. Monthly Posterior Fluxes

Posterior $FFCO_2$ emissions estimates from the inversion analysis also reflect the emissions decrease associated with the COVID-19 pandemic in both LA and DC-Balt (blue bars, Figure 2). In both March and April 2020, the posterior reflects significantly lower emissions than the inversion prior, and the April 2020 posterior is significantly lower than the posteriors for the pre-pandemic months in 2020 at 95% and 68% confidence intervals (CI) in LA (Figure 2c) and DC-Balt (Figure 2f), respectively. April 2020 posteriors are also lower than any other January through March period in the previous 2 years in both cities, suggesting that the decrease in this month is outside of seasonal and interannual variability. The posterior in March 2020 does not reflect as large a decrease as April, given that the reduction in activity due to the pandemic response occurred in mid-March in both cities.

In May 2020, the inversion $FFCO_2$ estimates are larger than those of April after accounting for uncertainties (Figures 2c and 2f). In LA, the May increase in the posterior emissions is likely due to the rebound in traffic given the second change point identified in Figure 1a. Alternatively, in DC-Balt, the standard deviation analysis did not indicate any clear change point associated with a recovery period possibly due to the large influence of the biosphere on atmospheric CO_2 in May (Figure 1d). In May, the biological contribution is nearly equal the $\mathbf{y}_{\mathbf{FFCO_2}}$ in DC-Balt (Figure S5c3), so any biases in the biological modeled fluxes would result in a bias in May posterior emissions. Unlike LA, we do not have a good measure on the uncertainty of these fluxes especially during the start of the growing season when representing the onset of photosynthetic uptake is difficult to model. Thus, in DC-Balt, we are not confident in attributing the increase in the posterior emissions in May 2020 to recovery response.

Beyond 2020, we further investigate the inversion posteriors to ensure that they are consistent with expected fluxes and trends for 2018, 2019, and 2020. The Hestia and Vulcan priors for LA and DC-Balt represent 2015 $FFCO_2$ emissions, and we expect emissions in each urban domain to be different in later years, especially in DC-Balt where emissions are more dependent on climate variability and where there have been substantial changes in the electricity sector over the last 5 years. To estimate a more representative year-specific domain total, we generate activity-based bottom-up (BU) estimates scaled from the Hestia and the Vulcan priors.

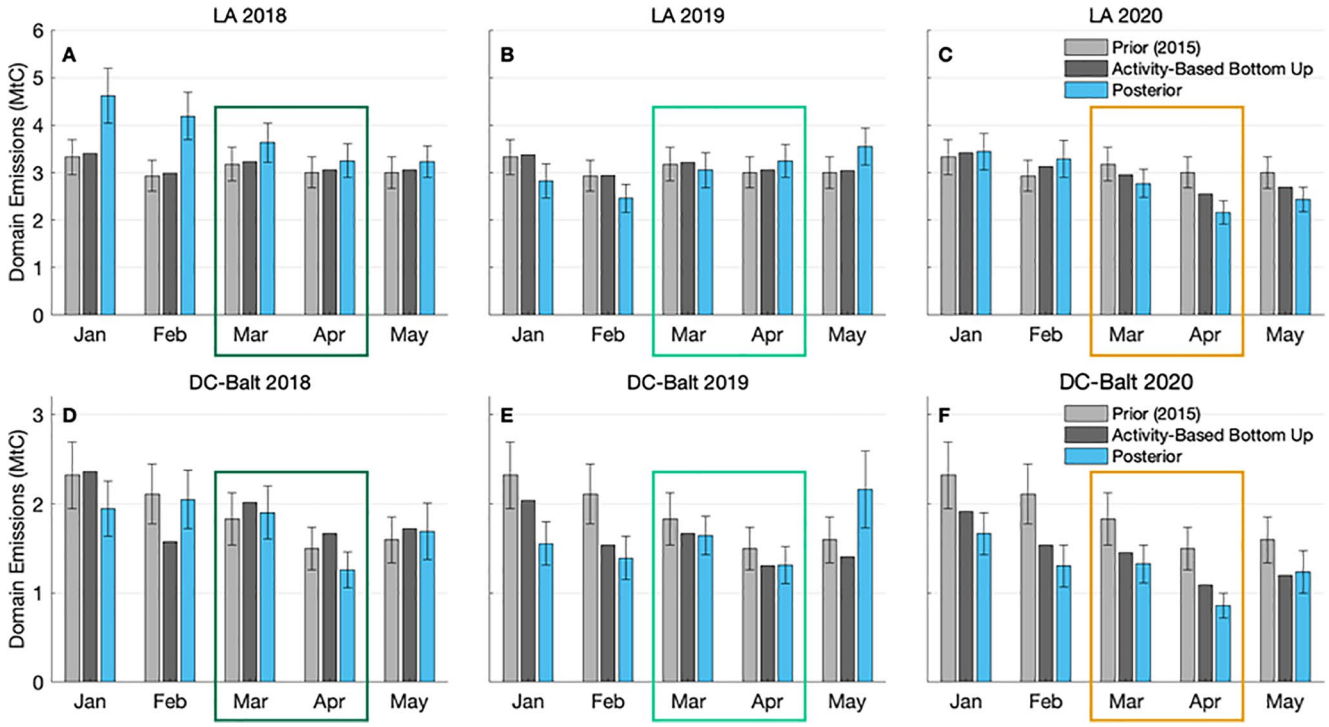

Figure 2. Inversion posterior monthly mean fossil-fuel CO_2 (FFCO2) emissions estimates for January–May 2018, 2019, and 2020, along with the 2015 prior emissions estimate (Hestia-LA: a–c; Vulcan: d–f) and an activity-based bottom-up (BU) estimate. Error bars on the posterior represent 95% confidence intervals. Uncertainties of the daily estimates are combined, accounting for correlations, to obtain overall uncertainties of the monthly means (Lawton, 2001). March and April are highlighted in each year with a colored rectangle. The error bars on the 2015 Hestia prior are 11% (Gurney et al., 2019) and for the 2015 Vulcan prior are 18% (Gurney et al., 2020).

For scaling, we use publicly available proxy data, such as reported emissions from electricity generation, natural gas usage, and fuel sales or VMT or vehicle hours traveled (VHT) (Section S8; Table S3). In DC-Balt and LA, all sectors contributing more than 10% of emissions in January through May were adjusted if public data was available. These year-specific estimates are not meant to provide accurate new emission products for these later years; rather, they provide a basis with which to compare our result for the whole-city domain (Figures 2a–2f, dark gray bars).

Overall, we find that the estimated $FFCO_2$ posteriors are often (but not always) more consistent with year-specific activity-based BU totals than with the 2015 prior. The general good comparison gives confidence in our posterior estimates and helps explain variability in the emission estimates between years. This improved consistency indicates that the CO_2 observations within the inversion are driving the estimated emissions to better represent the true emissions for a particular year or month.

For example, we expect more variability in posterior $FFCO_2$ emissions in DC-Balt than LA, largely due to climate. Indeed, in LA, the 2020 activity-based estimates are largely consistent with the 2015 prior for all months and years except for March, April, and May of 2020 (Figure 2, dark gray bars). The monthly variation in DC-Balt activity-based BU estimates is large from year to year because natural gas consumption to heat residential and commercial buildings largely depends on weather conditions in any given winter or spring. In addition, emissions from electricity production vary significantly between months and years in this region (Section S8). For example, the February 2019 activity-based BU emissions in DC-Balt are 27% lower than the 2015 prior and agree well with the posterior for that month (Figure 2e).

We note that the posterior LA emissions in January and February 2018 do not agree well with the activity-based BU emissions for these months (Figure 2a). The large posterior emissions in January 2018 may be caused by an active fire season in the region that stretched into the early days of 2018 (fire emissions are not included in the prior or activity-based BU estimates but would contribute to the posterior emissions as their signatures would be in $\mathbf{y}_{\mathbf{obs}}$). In February 2018, we suspect that poorly modeled meteorological

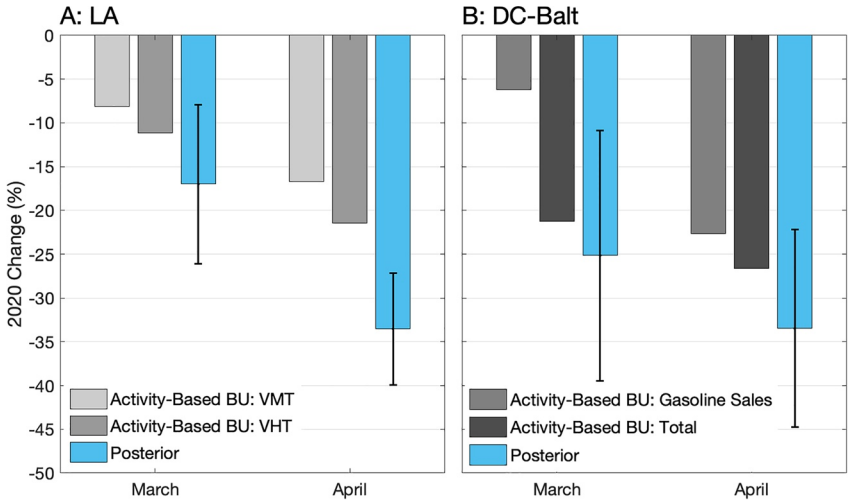

Figure 3. Changes in monthly mean emissions for April and March 2020 relative to 2018/2019 means for (a) LA and (b) DC-Balt. Blue bars represent the decrease estimated from the atmospheric inversion posteriors, with error bars representing the 95% CI. Various shades of gray bars represent the decrease for each month using different activity-based adjusted bottom-up totals, as indicated in the legend and described in the text.

conditions resulted in elevated emissions estimates, given the prevalence of low wind speeds in that month (Section S3.2).

7. Estimated Emissions Reductions

We compare March and April 2020 emissions to their respective means for 2018 and 2019 (Figure 3) to estimate the relative decrease in emissions in these months. We also compare the March and April activity-based BU totals for 2020 to those of previous years to discern whether the observed reductions are consistent with changes in activity data. In LA, in addition to VMT, we also calculate BU reductions using VHT data as a second point of comparison for the estimated relative reduction (Section S8.4). VHT decreased more than VMT during the pandemic because of reduced traffic congestion resulting in higher average vehicular speeds (Figure S11). We note that gasoline fuel sales, which is the best proxy data for on-road emissions, is only available at the state level, which may not reflect on-road activity in LA. We use both VMT and VHT in the analysis because they reflect different but related contributions to on-road emissions (distance traveled as well as time spent on the road).

In LA, the posterior reductions are 17% ± 9% (0.57 MtC ± 0.30 MtC, 95% CI) in March and 34% ± 6% (1.09 MtC ± 0.21 MtC, 95% CI) in April (blue bars, Figure 3). We also estimate a 28% ± 4% CO_2 emissions reduction for May in LA (not shown). The LA activity-based BU total for March and April suggests CO_2 emission reductions of 8% and 17%, respectively, all attributed to changes in VMT (light gray, Figure 3a). Using VHT, the reductions are slightly larger at 11% and 21%, which are smaller than the posterior estimates; these are within our estimated 95% CI in March but not in April (medium gray, Figure 3a). Overall, VMT/VHT in the LA area decreased by 17%/23% in March and 33%/42% in April 2020 compared to the mean of 2018 and 2019. Although VHT indicates a larger decrease than VMT (Figure S11), VMT has been previously used to estimate emissions from on-road vehicles (Gately et al., 2015; Gurney et al., 2020). The industrial sector is the only other significant portion of LA's total emissions, at 23%. There are some indications that this sector was impacted by COVID-19 or other external forces (e.g., significant labor drops in employment for the manufacturing sector) (Bureau of Labor Statistics, 2020; California Energy Commission, 2020; Hydrocarbon Processing, 2020). However, without a reliable proxy for the industrial sector, we are unable to account for any quantitative changes.

In DC-Balt, we estimate a slightly larger relative drop in the posterior emissions than in LA in March, that is, 25% ± 14% (0.45 MtC ± 0.25 MtC, 95% CI), while the April decrease is similar to LA, at 33% ± 11% (0.43 MtC ± 0.15 MtC, 95% CI) (blue bars, Figure 3b). The estimated decrease for both months is broadly

consistent with (although slightly larger than) the reductions predicted using the activity-based BU totals, which are 21% and 27% in March and April, respectively. However, only a 6% decrease in March is attributable to a reduction in the on-road sector relative to previous years, since only half of this month was affected by the slowdown in activity (medium gray bars, Figure 3b). The remainder of the 21% March BU decrease is largely attributed to reduced natural gas use in the residential and commercial sectors due to decreased demand for heating, as March 2020 was warmer than March 2018 and 2019. Natural gas use in DC-Balt was not anomalous in 2020 after accounting for regional temperatures and follows the trend with heating degree days from previous years (Figure S10), suggesting that behavioral changes due to COVID-19 were not responsible for the decline. In April 2020, the activity data suggest that most of the observed emissions reduction is indeed from on-road emissions, which are responsible for an estimated 23% decrease.

8. Conclusions

The response to COVID-19 influenced CO_2 emissions in both Los Angeles and Washington DC/Baltimore, resulting in declines of over 30% in April relative to previous years. These reductions are consistent with a 30% emissions decline found in the San Francisco Bay area between the 6 weeks prior and the 6 weeks after that city's lockdown (Turner et al., 2020). Our study demonstrates the detection of changes in urban-scale CO_2 emissions as small as 15%–30% during this time period. Overall, the atmospheric inversion-derived CO_2 emissions displayed significant drops in both cities due to factors (e.g., decreased traffic) impacted by COVID-19. Our three observation-based analyses allowed us to detect the timing of emissions declines, assess the continuation of reduced emissions, and estimate the relative change in emissions in March and April 2020 in comparison to 2018 and 2019. Beyond the reductions of CO_2 emissions due to COVID-19 impacts, we also found other factors that significantly influence monthly emissions using trends in publicly available activity data. In DC-Balt, both COVID-related traffic reduction and warmer weather caused the observed emissions decline; in LA, only a portion of the decline is attributable to a reduction in traffic, while some of the emissions declines remains unexplained.

The methods used here show that emission changes (whether due to pandemic effects, as shown here, or any other cause) that may be missed with solely an activity-based approach can be detected using atmospheric measurements. Such timely emissions information allows cities to assess the effectiveness of policies designed to reduce emissions. Furthermore, accurate CO_2 emissions information provided at shorter timescales could be crucial to policy makers to course-correct their mitigation actions if necessary and propose new measures (e.g., redesigning transportation infrastructure) that will ultimately drive down CO_2 emissions.

Data Availability Statement

All data used in this analysis are available at data.nist.gov (https://doi.org/10.18434/mds2-2343).

Acknowledgments
The authors thank Hratch Semerjian and Eleanor Waxman (NIST), Michael Stock, Elizabeth DiGangi, Bryan Biggs, and Charlie Draper (EN) for their contributions. This work was partially funded by NIST grants 70NANB15H344, 70NANB14H322, 70NANB19H129, 70NANB19H130, 70NANB19H132, along with a commercial contract with EN (1333ND-19PNB600853). A portion of this research was carried out at the Jet Propulsion Laboratory, California Institute of Technology, under a contract with the National Aeronautics and Space Administration (80NM0018D0004).

References

Aminikhanghahi, S., & Cook, D. J. (2017). A survey of methods for time series change point detection. *Knowledge and Information Systems*, *51*(2), 339–367. https://doi.org/10.1007/s10115-016-0987-z

Apple (2020). *Mobility trends reports*. Retrieved from https://covid19.apple.com/mobility

Bureau of Labor Statistics (2020). *Occupational employment and Wages in Los Angeles-Long Beach-Anaheim, state and area employment, hours, and earnings*. Retrieved from https://data.bls.gov/timeseries/SMS06000003000000001?amp%253bdata_tool=XGtable&output_view=data&include_graphs=true

California Dept. of Transportation (2020). *Caltrans performance measurement system (PeMS)*. Retrieved from http://pems.dot.ca.gov

California Energy Commission (2020). *Energy Insights August 2020*. Retrieved from https://www.energy.ca.gov/sites/default/files/2020-08/Energy%20Insights_2020-08_ada.pdf

Gately, C. K., Hutyra, L. R., & Sue Wing, I. (2015). Cities, traffic, and CO_2: A multidecadal assessment of trends, drivers, and scaling relationships. *Proceedings of the National Academy of Sciences of the United States of America*, *112*(16), 4999–5004. https://doi.org/10.1073/pnas.1421723112

Gurney, K. R., Liang, J., Patarasuk, R., Song, Y., Huang, J., & Roest, G. (2020). The Vulcan version 3.0 high-resolution fossil fuel CO_2 emissions for the United States. *Journal of Geophysical Research: Atmospheres*, *125*(19). https://doi.org/10.1029/2020JD032974

Hydrocarbon Processing (2020). *Marathon Los Angeles Refinery cuts production due to demand drop*. Retrieved from https://www.hydrocarbonprocessing.com/news/2020/03/marathon-los-angeles-refinery-cuts-production-due-to-demand-drop

Karion, A., Callahan, W., Stock, M., Prinzivalli, S., Verhulst, K. R., Kim, J., et al. (2020). Greenhouse gas observations from the Northeast Corridor tower network. *Earth System Science Data*, *12*(1), 699–717. https://doi.org/10.5194/essd-12-699-2020

Karion, A., Lopez-Coto, I., Gourdji, S. M., Mueller, K., Ghosh, S., Callahan, W., et al. (2021). Background conditions for an urban greenhouse gas network in the Washington, D.C. and Baltimore metropolitan region. *Atmospheric Chemistry and Physics*, *21*(8), 6257–6273. https://doi.org/10.5194/acp-21-6257-2021

Kort, E. A., Angevine, W. M., Duren, R., & Miller, C. E. (2013). Surface observations for monitoring urban fossil fuel CO_2 emissions: Minimum site location requirements for the Los Angeles megacity. *Journal of Geophysical Research: Atmospheres*, *118*, 1577–1584. https://doi.org/10.1002/jgrd.50135

Lawton, R. (2001), Time series analysis and its applications, *International Journal of Forecasting*, *17*, 299–301. https://doi.org/10.1016/s0169-2070(01)00083-8

Le Quéré, C., Jackson, R. B., Jones, M. W., Smith, A. J. P., Abernethy, S., Andrew, R. M., et al. (2020). Temporary reduction in daily global CO_2 emissions during the COVID-19 forced confinement. *Nature Climate Change*, *10*(7), 647–653. https://doi.org/10.1038/s41558-020-0797-x

Liu, Z., Ciais, P., Deng, Z., Lei, R., Davis, S. J., Feng, S., et al. (2020). Near-real-time monitoring of global CO_2 emissions reveals the effects of the COVID-19 pandemic. *Nature Communications*, *11*, 1–12. https://doi.org/10.1038/s41467-020-18922-7

Lopez-Coto, I., Ghosh, S., Prasad, K., & Whetstone, J. (2017). Tower-based greenhouse gas measurement network design—The national institute of standards and technology north east Corridor testbed. *Advances in Atmospheric Sciences*, *34*(9), 1095–1105. https://doi.org/10.1007/s00376-017-6094-6

Miller, J. B., Lehman, S. J., Verhulst, K. R., Miller, C. E., Duren, R. M., Yadav, V., et al. (2020). Large and seasonally varying biospheric CO_2 fluxes in the Los Angeles megacity revealed by atmospheric radiocarbon. *Proceedings of the National Academy of Sciences of the United States of America*, *117*(43), 26681–26687. https://doi.org/10.1073/pnas.2005253117

Mueller, K., V., Yadav, I., Lopez-Coto, A., Karion, S., Gourdji, C., Martin, & J. Whetstone. (2018), Siting background towers to characterize incoming air for Uuban Greenhouse gas estimation A case study in the Washington, DC/Baltimore area, *Journal of Geophysical Research Atmospheres*, *123*(5), 2910–2926. https://doi.org/10.1002/2017JD027364

Sargent, M., Barrera, Y., Nehrkorn, T., Hutyra, L. R., Gately, C. K., Jones, T., et al. (2018). Anthropogenic and biogenic CO_2 fluxes in the Boston urban region. *Proceedings of the National Academy of Sciences of the United States of America*, *115*(29), 7491–7496. https://doi.org/10.1073/pnas.1803715115

Turner, A. J., Kim, J., Fitzmaurice, H., Newman, C., Worthington, K., Chan, K., et al. (2020). Observed impacts of COVID-19 on urban CO_2 Emissions. *Geophysical Research Letters*, *47*(22), e2020GL090037. https://doi.org/10.1029/2020GL090037

Umezawa, T., Matsueda, H., Oda, T., Higuchi, K., Sawa, Y., Machida, T., et al. (2020). Statistical characterization of urban CO_2 emission signals observed by commercial airliner measurements. *Scientific Reports*, *10*(1), 7963. https://doi.org/10.1038/s41598-020-64769-9

US Census (2010). *US census urban areas.* Retrieved from https://www.census.gov/programs-surveys/geography/guidance/geo-areas/urban-rural/2010-urban-rural.html

Verhulst, K. R., Karion, A., Kim, J., Salameh, P. K., Keeling, R. F., Newman, S., et al. (2017). Carbon dioxide and methane measurements from the Los Angeles Megacity Carbon Project - Part 1: Calibration, urban enhancements, and uncertainty estimates. *Atmospheric Chemistry and Physics*, *17*(13), 8313–8341. https://doi.org/10.5194/acp-17-8313-2017

Zheng, B., Geng, G., Ciais, P., Davis, S. J., Martin, R. V., Meng, J., et al. (2020). Satellite-based estimates of decline and rebound in China's CO_2 emissions during COVID-19 pandemic. *Science Advances*, *6*(49), eabd4998. https://doi.org/10.1126/sciadv.abd4998

References From the Supporting Information

Angevine, W. M., Eddington, L., Durkee, K., Fairall, C., Bianco, L., & Brioude, J. (2012). Meteorological model evaluation for CalNex 2010. *Monthly Weather Review*, *140*(12), 3885–3906. https://doi.org/10.1175/mwr-d-12-00042.1

Bagley, J. E., Jeong, S., Cui, X., Newman, S., Zhang, J., Priest, C., et al. (2017), Assessment of an atmospheric transport model for annual inverse estimates of California greenhouse gas emissions, *Journal of Geophysical Research: Atmospheres*, *122*(3), 1901–1918. https://doi.org/10.1002/2016JD025361

Benjamin, S. G., Weygandt, S. S., Brown, J. M., Hu, M., Alexander, C. R., Smirnova, T. G., et al. (2016). A north American hourly assimilation and model forecast cycle: The rapid refresh. *Monthly Weather Review*, *144*(4), 1669–1694. https://doi.org/10.1175/mwr-d-15-0242.1

Chevallier, F., & O'Dell, C. W. (2013). Error statistics of Bayesian CO_2 flux inversion schemes as seen from GOSAT. *Geophysical Research Letters*, *40*(6), 1252–1256. https://doi.org/10.1002/grl.50228

Christenson, M., Manz, H., & Gyalistras, D. (2006). Climate warming impact on degree-days and building energy demand in Switzerland. *Energy Conversion and Management*, *47*(6), 671–686. https://doi.org/10.1016/j.enconman.2005.06.009

Coleman, R. W., Stavros, N., Yadav, V., & Parazoo, N. (2020). A simplified framework for high-resolution urban vegetation classification with optical imagery in the Los Angeles Megacity. *Remote Sensing*, *12*(15), 2399. https://doi.org/10.3390/rs12152399

D'Amico, A., Ciulla, G., Panno, D., & Ferrari, S. (2019). Building energy demand assessment through heating degree days: The importance of a climatic dataset. *Applied Energy*, *242*, 1285–1306. https://doi.org/10.1016/j.apenergy.2019.03.167

Deng, F., Chen, J. M., Ishizawa, M., Yuen, C.-W., Mo, G., Higuchi, K., et al. (2007). Global monthly CO_2 flux inversion with a focus over North America. *Tellus B: Chemical and Physical Meteorology*, *59*(2), 179–190. https://doi.org/10.1111/j.1600-0889.2006.00235.x

De Rosa, M., Bianco, V., Scarpa, F., & Tagliafico, L. A. (2014). Heating and cooling building energy demand evaluation; a simplified model and a modified degree days approach. *Applied Energy*, *128*, 217–229. https://doi.org/10.1016/j.apenergy.2014.04.067

EPA (2020). *Air markets program data*. Retrieved from https://ampd.epa.gov/ampd/

Feng, S., Lauvaux, T., Newman, S., Rao, P., Ahmadov, R., Deng, A., et al. (2016). Los Angeles megacity: A high-resolution land-atmosphere modeling system for urban CO_2 emissions. *Atmospheric Chemistry and Physics*, *16*(14), 9019–9045. https://doi.org/10.5194/acp-16-9019-2016

Gurney, K. R., Liang, J., Patarasuk, R., Song, Y., Huang, J., & Roest, G. (2020). *Vulcan: High-resolution annual fossil fuel CO_2 emissions in USA, 2010–2015*. ORNL Distributed Active Archive Center. https://doi.org/10.3334/ORNLDAAC/1741

Gurney, K. R., Patarasuk, R., Liang, J., Song, Y., O'Keeffe, D., Rao, P., et al. (2019). The Hestia fossil fuel CO_2 emissions data product for the Los Angeles megacity (Hestia-LA). *Earth System Science Data*, *11*(3), 1309–1335. https://doi.org/10.5194/essd-11-1309-2019

Gurney, K. R., Roest, G., Liang, J., Darragh, O. K., Huang, J., Song, Y., et al. (2018). *Hestia fossil fuel carbon dioxide emissions inventory for Los Angeles basin*. National Institute of Standards and Technology. https://doi.org/10.18434/T4/1502503

Karion, A., Lauvaux, T., Lopez Coto, I., Sweeney, C., Mueller, K., Gourdji, S., et al. (2019). Intercomparison of atmospheric trace gas dispersion models: Barnett Shale case study. *Atmospheric Chemistry and Physics*, *19*(4), 2561–2576. https://doi.org/10.5194/acp-19-2561-2019

Kitanidis, P. K. (1995). Quasi-Linear geostatistical theory for inversing. *Water Resources Research*, *31*(10), 2411–2419. https://doi.org/10.1029/95wr01945

Kohler, M., Blond, N., & Clappier, A. (2016). A city scale degree-day method to assess building space heating energy demands in Strasbourg Eurometropolis (France). *Applied Energy*, *184*, 40–54. https://doi.org/10.1016/j.apenergy.2016.09.075

Lauvaux, T., Pannekoucke, O., Sarrat, C., Chevallier, F., Ciais, P., Noilhan, J., & Rayner, P. J. (2009). Structure of the transport uncertainty in mesoscale inversions of CO_2 sources and sinks using ensemble model simulations. *Biogeosciences*, *6*(6), 1089–1102. https://doi.org/10.5194/bg-6-1089-2009

Lin, J. C., Gerbig, C., Wofsy, S. C., Andrews, A. E., Daube, B. C., Davis, K. J., & Grainger, C. A. (2003). A near-field tool for simulating the upstream influence of atmospheric observations: The Stochastic Time-Inverted Lagrangian Transport (STILT) model. *Journal of Geophysical Research*, *108*(D16), 4493. https://doi.org/10.1029/2002jd003161

Lindeløv, J. K. (2020). *mcp: An R package for regression with multiple change points*. OSF Preprints. https://doi.org/10.31219/osf

Mahadevan, P., Wofsy, S. C., Matross, D. M., Xiao, X., Dunn, A. L., Lin, J. C., et al. (2008). A satellite-based biosphere parameterization for net ecosystem CO_2 exchange: Vegetation Photosynthesis and Respiration Model (VPRM). *Global Biogeochemical Cycles*, *22*(2), GB2005. https://doi.org/10.1029/2006gb002735

Michalak, A. M., Hirsch, A., Bruhwiler, L., Gurney, K. R., Peters, W., & Tans, P. P. (2005). Maximum likelihood estimation of covariance parameters for Bayesian atmospheric trace gas surface flux inversions. *Journal of Geophysical Research*, *110*(D24), 16. https://doi.org/10.1029/2005jd005970

National Weather Service (2020). *Heating and Cooling degree days*. Retrieved from https://www.weather.gov/key/climate_heat_cool

NDCD (2020). *NCDC monthly HDD data for Maryland*. Retrieved from https://www.cpc.ncep.noaa.gov/products/analysis_monitoring/cdus/degree_days/

Park, C., Gerbig, C., Newman, S., Ahmadov, R., Feng, S., Gurney, K. R., et al. (2018). CO_2 transport, variability, and budget over the Southern California air basin using the high-resolution WRF-VPRM model during the CalNex 2010 campaign. *Journal of Applied Meteorology and Climatology*, *57*(6), 1337–1352. https://doi.org/10.1175/JAMC-D-17-0358.1

Sweeney, C., Karion, A., Wolter, S., Newberger, T., Guenther, D., Higgs, J. A., et al. (2015). Seasonal climatology of CO_2 across north America from aircraft measurements in the NOAA/ESRL Global Greenhouse Gas Reference Network. *Journal of Geophysical Research: Atmospheres*, *120*(10), 5155–5190. https://doi.org/10.1002/2014jd022591

Tarantola, A. (2005). *Inverse Problem Theory and Methods for Model Parameter Estimation*. SIAM. https://doi.org/10.1137/1.9780898717921

U.S. EIA (2020a). *Monthly, state-level "Natural gas consumption by end use" for DC*. Retrieved from https://www.eia.gov/dnav/ng/NG_CONS_SUM_DCU_SDC_M.htm

U.S. EIA (2020b). *Monthly, state-level "Natural gas consumption by end use" for Maryland*. Retrieved from https://www.eia.gov/dnav/ng/NG_CONS_SUM_DCU_SMD_M.htm

U.S. EIA (2020c). *Monthly, state-level "Natural gas consumption by end use" for Virginia*. Retrieved from https://www.eia.gov/dnav/ng/NG_CONS_SUM_DCU_SVA_M.htm

U.S. EIA (2020d). *Monthly, state-level "Prime supplier sales volumes" for "motor gasoline" for DC*. Retrieved from https://www.eia.gov/dnav/pet/pet_sum_mkt_dcu_sDC_m.htm

U.S. EIA (2020e). *Monthly, state-level "Prime supplier sales volumes" for "motor gasoline" for Maryland*. Retrieved from https://www.eia.gov/dnav/pet/pet_sum_mkt_dcu_sMD_m.htm

U.S. EIA (2020f). *Monthly, state-level "Prime supplier sales volumes" for "motor gasoline" for Virginia*. Retrieved from https://www.eia.gov/dnav/pet/pet_sum_mkt_dcu_sVA_m.htm

Ware, J., Kort, E. A., Duren, R., Mueller, K. L., Verhulst, K., & Yadav, V. (2019). Detecting urban emissions changes and events with a near-real-time-capable inversion system. *Journal of Geophysical Research: Atmospheres*, *124*(9), 5117–5130. https://doi.org/10.1029/2018jd029224

Yadav, V., Duren, R., Mueller, K., Verhulst, K. R., Nehrkorn, T., Kim, J., et al. (2019). Spatio-temporally resolved methane fluxes from the Los Angeles Megacity. *Journal of Geophysical Research: Atmospheres*, *124*(9), 5131–5148. https://doi.org/10.1029/2018jd030062

Zinzi, M., Carnielo, E., & Mattoni, B. (2018). On the relation between urban climate and energy performance of buildings. A three-years experience in Rome, Italy. *Applied Energy*, *221*, 148–160. https://doi.org/10.1016/j.apenergy.2018.03.192